WHIOCE PUBLISHING PTE. LTD.
PROVIDING
FIRST-CLASS SCIENTIFIC INFORMATION
FOR TOP SCHOLARS

2025 Volume 10, Issue 4
Journal of Medicines Development Sciences
ISSN: 2382-6371(Online) ISSN: 2382-6363(Print)

10-Deacetylbaccatin III Alleviates Inflammation by Inhibiting NF-κB in the Joints of AIA Mice

Jiabao Gan, Yue Gao, Ke Yang, Ye He, Guangchen Sun*
Guilin Medical University, Guiling 541000, Guangxi, China

**Author to whom correspondence should be addressed.*

Abstract: *Objective:* To evaluate the therapeutic potential of 10-deacetylbaccatin III (10-DAB) in rheumatoid arthritis (RA) and to determine whether its anti-inflammatory effects are mediated through inhibition of the NF-κB signaling pathway. *Methods:* CFA-induced AIA mice received vehicle, 10-DAB (30 or 120 mg kg^{-1}) or DEX for 28 d; paw swelling, clinical score and body weight were recorded every 48 h. Knees were stained (H&E/TRAP) for synovitis and osteoclasts; serum cytokines (TNF-α, IL-6, IL-10) were quantified by ELISA; spleen p-p65, p-IκBα, iNOS and MMP-3 by Western blot. LPS-stimulated RAW264.7 macrophages were treated with 10-DAB or DEX; viability (CCK-8) and NF-κB activation were assessed. *Results:* 10-DAB dose-dependently alleviated paw swelling and clinical scores, preserved cartilage and decreased TRAP-positive osteoclasts. It significantly decreased serum TNF-α/IL-6, elevated IL-10, suppressed IκBα/p65 phosphorylation, blocked p65 nuclear import and down-regulated iNOS/MMP-3 in spleen. In RAW264.7 cells, non-toxic 10-DAB inhibited LPS-induced IκBα/p65 phosphorylation and TNF-α release. *Conclusion:* 10-DAB ameliorates AIA by blocking the NF-κB cascade and downstream inflammatory mediator production, indicating its potential as a candidate for RA therapy.

Keywords: 10-Deacetylbaccatin III; adjuvant-induced arthritis; NF-κB; inflammatory factors; rheumatoid arthritis

Online publication: December 26, 2025

1. Introduction

Rheumatoid arthritis (RA) is a systemic autoimmune disease characterized by chronic synovitis and progressive joint destruction, with a global prevalence of approximately 1%, imposing a significant burden on patients and society [1]. The pathological process of RA is extremely complex, involving abnormal activation and interaction of various immune cells, including infiltrating T cells, B cells, neutrophils, as well as resident synovial fibroblasts and macrophages. Among them, macrophages, as core effector cells of innate immunity, play a crucial role in the initiation and sustained progression of RA [2]. Activated macrophages extensively infiltrate into the synovial tissue, producing and releasing a large amount of pro-inflammatory cytokines (such as TNF-α, IL-1β, IL-6) and matrix metalloproteinases (MMPs), directly driving local inflammation amplification, synovial hyperplasia, and leading to cartilage and bone erosion [3]. Despite significant progress in the application of biologics and targeted synthetic disease-modifying antirheumatic drugs (DMARDs), some patients still exhibit poor efficacy or face severe side effects [4]. Therefore, exploring novel anti-inflammatory drugs from natural products that can effectively regulate the function of key immune cells such as macrophages remains a focus of current

research.

In the complex inflammatory network of RA, the NF-κB signaling pathway plays a vital and central role, serving as the core signaling hub for the production of pro-inflammatory factors by immune cells such as macrophages. NF-κB is a key transcription factor that regulates the expression of numerous genes involved in inflammation, immune responses, and cell survival [5]. Core members of the classical NF-κB pathway include the p65 (RelA) subunit and its inhibitory protein IκBα. In the resting state, p65 forms a dimer with p50 and binds to IκBα, being anchored in an inactive form in the cytoplasm [6]. When macrophages and other cells are stimulated by pro-inflammatory factors such as tumor necrosis factor-α (TNF-α) and lipopolysaccharide (LPS), the IκB kinase (IKK) complex is activated. Activated IKK subsequently phosphorylates specific serine residues (such as Ser32/36) of IκBα, generating p-IκBα. p-IκBα is rapidly ubiquitinated and degraded via the proteasome pathway, thereby relieving the inhibition on NF-κB. The released p65/p50 dimer then undergoes nuclear translocation [7]. During this process, the p65 subunit itself is also phosphorylated at sites such as Ser536, forming p-p65, a step that further enhances its transcriptional activity and stability. After entering the nucleus, p-p65 binds to specific DNA sequences, initiating the gene transcription of a large number of pro-inflammatory mediators and enzymes such as TNF-α, IL-1β, IL-6, COX-2, and MMPs, thereby sharply amplifying and sustaining the inflammatory response [8]. Sustained abnormal activation of the NF-κB pathway can be observed in the synovial tissue of RA patients and the joints of adjuvant-induced arthritis (AIA) model mice, indicating that targeted inhibition of this pathway is an effective strategy for regulating macrophage function and alleviating RA inflammation.

10-Deacetylbaccatin III (10-DAB) can be isolated from the dry needles and twigs of *Taxus baccata* and is an important raw material for the synthesis of anticancer drugs paclitaxel and docetaxel [9]. 10-DAB is mainly extracted from the branches and leaves of Taxus plants. Studies have shown that as a naturally occurring small-molecule compound, 10-DAB has been found to possess various biological activities in recent years, including anti-parasitic, anti-inflammatory, antioxidant, and immunomodulatory effects [10-12]. These properties make it a potential candidate drug for studying RA treatment strategies. However, the specific mechanism by which 10-DAB exerts its anti-inflammatory effects and thus affects the course of RA remains unclear.

The AIA model is a classic and reliable animal model for studying RA. Its characteristics lie in simulating the core pathological features of human RA: triggering strong acute inflammation, chronic synovial hyperplasia, massive infiltration of inflammatory cells, and progressive cartilage and bone destruction, accompanied by significant splenomegaly and elevated levels of serum pro-inflammatory cytokines (such as TNF-α, IL-6), with a pronounced systemic immune response [13,14]. In this study, by establishing an AIA mouse model, we systematically evaluated the therapeutic effect of 10-DAB on arthritis and explored its molecular mechanism, providing a basis for the development of natural anti-RA drugs.

Based on the above background, this study aims to systematically investigate the therapeutic effect of 10-DAB on the AIA mouse model and delve into whether its molecular mechanism is related to the inhibition of the NF-κB signaling pathway, particularly its role in regulating macrophage function.First, by establishing an AIA mouse model, we evaluated in vivo the improvement effects of 10-DAB on arthritis score, paw swelling, and joint tissue pathological damage. The spleen is the largest peripheral immune organ, rich in various immune cells such as T cells, B cells, macrophages, and dendritic cells [15]. In systemic autoimmune disease models such as CFA-induced AIA,The spleen serves as a key site for the activation and proliferation of immune cells(including macrophages), as well as a pivotal hub for the initiation of systemic inflammatory responses. Therefore, we used Western blotting (WB) to detect the expression and activation of key proteins in the NF-κB pathway in the spleen tissue of AIA mice. In RA, activated NF-κB directly initiates the transcription of iNOS through nuclear translocation, leading to the production of a large amount of nitric oxide (NO), exacerbating the inflammatory response and tissue damage. Meanwhile, the upregulation of NF-κB also directly promotes the expression of MMP-3, which can degrade key components (such as proteoglycans and laminin) in the cartilage matrix and is one of the main causes of joint structural destruction [16]. We focused on analyzing changes in p65 nuclear translocation, p-p65 (Ser536), and p-IκBα levels to preliminarily verify the in vivo target of 10-DAB.

To further confirm the direct effect of 10-DAB on macrophages and its mechanism at the cellular level, we extended

our research system to in vitro experiments. RAW 264.7 cells are derived from a mouse monocyte-macrophage cell line and are key effector cells in the inflammatory response, commonly used to simulate the behavior of macrophages in vivo. LPS is the main component of the cell wall of Gram-negative bacteria. It can activate a series of inflammatory signaling pathways within cells by binding to Toll-like receptor 4 (TLR4) on the macrophage surface, efficiently and reproducibly simulating macrophage activation under bacterial infection or inflammatory conditions [17]. We used LPS to stimulate RAW264.7 cells to simulate an in vitro inflammatory environment and observed the effect of 10-DAB pretreatment on the expression of inflammation factors induced by LPS. Simultaneously, we will again detect the phosphorylation and degradation of p65 and IκBα in the cells, as well as changes in the expression level of TNF-α in the cell culture medium, thereby confirming at a more precise level whether 10-DAB directly acts on key nodes of the NF-κB pathway in macrophages, inhibits the phosphorylation of IκBα and p65, and ultimately blocks the expression of downstream inflammatory genes.

This study, through a combination of in vivo and in vitro experiments, focused on exploring the potential of 10-DAB to exert anti-RA effects by regulating the NF-κB signaling pathway in macrophages.It not only furnishes robust scientific evidence for the molecular mechanisms underlying 10-DAB's anti-arthritic activity, but also establishes a critical theoretical framework for its further development as a natural drug candidate against rheumatoid arthritis.

2. Materials And Methods

2.1. Reagents

10-DAB (CAS 32981-86-5, ≥98 % purity) was from Chengdu Lookchem Biotechnology Co., Ltd. (Chengdu, China); LPS (Escherichia coli O111:B4 lipopolysaccharide) was supplied by MedChemExpress (Monmouth Junction, NJ, USA); DMEM (Dulbecco's Modified Eagle Medium) and fetal bovine serum (FBS) were obtained from Gibco (Grand Island, NY, USA) and CLARK (Clayton, NC, USA), respectively; ELISA kits for IL-10, IL-6 and TNF-α were purchased from Wuhan Proteintech Biotechnology Co., Ltd. (Wuhan, China).

2.2. Experimental Animals

Thirty male KM mice (6–8 weeks, 25 ± 2 g) were supplied by Jiangsu GemPharmatech Co., Ltd. (license No. SCXK (Su) 2023-0009). After 1-week quarantine, they were kept in the specific-pathogen-free (SPF) barrier facility of the Guangxi Key Laboratory of Drug Molecular Discovery and Medicinal Property Optimization, College of Pharmacy, Guilin Medical University (license No. SYXK (Gui) 2022-0005). Room temperature was maintained at 22 ± 2 °C, relative humidity at 40–70 %. All procedures were approved by the Institutional Animal Care and Use Committee (IACUC) of Guilin Medical University (approval No. GLMU-IACUC-20251078) and conducted in accordance with the ARRIVE 2.0 guidelines.

2.3. Experimental design and arthritis induction

Thirty male KM mice were habituated for 7 days and then randomly allocated to five groups (n = 6) by stratified randomization based on baseline paw thickness.

Groups:(1)Control (Ctrl);(2) AIA model (AIA);(3) 10-DAB low-dose (10-DAB-L);(4) 10-DAB high-dose (10-DAB-H): 120 mg kg^{-1}, i.g;(5) Positive control (DEX): dexamethasone 0.5 mg kg^{-1}, i.g . Following a 3-day prophylactic regimen, arthritis was induced: mice were anaesthetized with 0.2 % pentobarbital sodium and given a sub-plantar injection of 0.1 ml CFA containing 4 mg ml^{-1} heat-killed Mycobacterium tuberculosis, whereas Control animals received an equal volume of saline. Paw, ankle and knee thickness of each mouse were measured before induction (Day 0). Thereafter, intragastric administration of the test agents was commenced on Day 2 post-induction and maintained at 48-hour intervals for 28 consecutive days; both Control and AIA cohorts were gavaged with the corresponding vehicle.

2.4. Observation Indicators

Prior to the induction of arthritis on Day 0, ankle joint edema was quantified in both the transverse and longitudinal planes with a digital thickness gauge (precision 0.001–10 mm). Thereafter, ankle swelling and body mass were recorded at 48-hour intervals. Three investigators independently evaluated the macroscopic appearance of each ankle for erythema, deformity, and eschar formation. Arthritis severity was graded according to a validated 5-point visual scale: 0 = no swelling or erythema; 1 = mild peri-articular swelling or erythema with digit inflammation; 2 = moderate swelling and erythema confined to the distal two-thirds of the paw; 3 = pronounced swelling and erythema extending to the ankle joint; 4 = severe diffuse swelling, erythema, and joint rigidity involving ankle, foot, and digits. Each limb was scored individually (range 0–4)[18], yielding a maximum cumulative score of 16 per animal. The final arthritis index was calculated as the arithmetic mean of the three independent observer scores.

2.5. Cell Culture and Treatment

Murine RAW264.7 macrophages (Wuhan Zishan Biotechnology, Wuhan, China; catalog no. STCC20020) were maintained in Dulbecco's modified Eagle's medium (DMEM; Gibco, Grand Island, NY, USA) supplemented with 10 %fetal bovine serum (FBS; Gibco) and 1 % penicillin–streptomycin at 37 °C in a humidified 5 % CO_2 atmosphere. For experiments, cells were seeded at 5×10^5 cells per 6-cm dish and grown to ≈ 50 % confluence. After 24 h, the medium was replaced with serum-free DMEM for an additional 24 h. Thereafter, cells were pre-treated with 10-DAB (10 μM; Sigma-Aldrich, St. Louis, MO, USA) or vehicle (0.1 % DMSO) for 4 h, followed by stimulation with lipopolysaccharide (LPS; 500 ng ml^{-1}, Escherichia coli O111:B4; Sigma-Aldrich) for 24 h. Culture supernatants and cell pellets were then harvested and stored at −80 °C until further analysis.

2.6. Western Bloting

Spleen samples were snap-frozen in liquid nitrogen and homogenised in RIPA buffer (Beyotime, Shanghai, China) supplemented with 1 mM PMSF and 1 % phosphatase inhibitor cocktail (Sigma-Aldrich). After 12 000 × g centrifugation (4 °C, 15 min), supernatant protein concentrations were determined with a BCA kit (Thermo Fisher Scientific). Equal amounts of protein (20 μg per lane) were resolved on 10 % SDS-PAGE gels and electro-transferred (100 V, 90 min) to 0.22 μm PVDF membranes (Millipore). Membranes were blocked with fast-blocking buffer (Beyotime) for 15 min at room temperature (RT) and incubated overnight at 4 °C with the following primary antibodies: anti-p65 (1:10 000; Abcam), anti-phospho-p65 (Ser536, 1:10 000; Abcam), anti-IκBα (1:10 000; Abcam), anti-phospho-IκBα (Ser32/36, 1:2000; Wanleibio), anti-iNOS (1:2000; Wanleibio) and anti-MMP-3 (1:1000; Servicebio). After three 5-min washes with TBST, membranes were probed with HRP-conjugated secondary antibodies (1:5000; ZSGB-Bio) for 1 h at RT. Immunoreactive bands were visualized using an ECL substrate (Bio-Rad) and quantified with ImageJ software (NIH, USA); GAPDH (1:20000; Proteintech) served as the loading control.

Cells were rinsed twice with ice-cold PBS and lysed in RIPA buffer (Beyotime) containing 1 mM PMSF and 1 % phosphatase inhibitor cocktail (Sigma-Aldrich) for 30 min on ice. After clarification (12000×g, 4 °C, 15 min), protein concentrations were quantified with a BCA kit (Thermo Fisher Scientific). Equal loads (20 μg per lane) were resolved on 10 % SDS-PAGE gels and electro-transferred to 0.22 μm PVDF membranes (Millipore). Blocking, antibody incubation and chemiluminescent detection were performed exactly as described for splenic tissue. The NF-κB cascade was probed with anti-p65 (1:10 000; Abcam, ab32536), anti-phospho-p65 (Ser536, 1:10 000; Abcam, ab76302), anti-IκBα (1:10 000; Abcam, ab32518) and anti-phospho-IκBα (Ser32/36, 1:2000; Wanleibio, WL01951).

2.7. ELISA

Mouse serum and the supernatant of macrophage culture medium were collected. The levels of IL-10, IL-6, and TNF-α were determined using the double-sandwich ELISA method. All samples were assayed in triplicate and data from three independent experiments were pooled for statistical analysis.

2.8. Statistical Analysis

Statistical analyses were performed with SPSS 20.0 (IBM, Armonk, NY, USA) and graphs were generated in GraphPad Prism 8 (GraphPad Software, San Diego, CA, USA). Data are expressed as mean ± SEM of at least three independent experiments. Statistical analysis of the data was carried out using t-tests, one-way analysis of variance (ANOVA), and non-parametric tests. Significance levels are denoted as #P < 0.05, ##P < 0.01 and ###P < 0.001 versus the normal group, and *P < 0.05, **P < 0.01 and ***P < 0.001 versus the model group.

3. Results

3.1. 10-DAB reduces the degree of arthritis swelling, clinical scores, and spleen index in AIA mice

To evaluate the therapeutic effect of 10-DAB on the AIA mouse model, this study systematically monitored the progression of arthritis in mice and the intervention effect of 10-DAB. After the model was established, we dynamically tracked the development of joint inflammation by measuring changes in the thickness of the hindlimb paws and ankle joints of the mice. On Day 30, we euthanized all the mice and recorded the final arthritis symptoms on the day of euthanasia (**Figure 1A**).

At the end of the experiment, detailed clinical inflammatory scores were assigned to the joints of all mice according to pre-set criteria. The results showed that the mice in the Control group did not exhibit significant redness or swelling in the hindlimbs throughout the experimental period and remained in good condition. In stark contrast, mice in the AIA group, L-10-DAB group, H-10-DAB group, and DEX group began to show obvious swelling in the hindlimb joints starting from the 3rd day after model establishment. This swelling condition continued to worsen over time and reached its peak of inflammation on the 16th day after model establishment, when the average arthritis score of the model group was as high as 5.62 ± 1.32 (**Figure 1B**).

Compared with the AIA group, mice in the H-10-DAB group showed significant improvement in arthritis. Specifically, there was a significant reduction in paw swelling (P < 0.01), indicating effective control of local inflammation. The clinical arthritis score also decreased significantly, with a reduction of over 50%, which directly reflected a marked alleviation of symptoms such as joint redness and swelling. In addition, the spleen index measured at the end of the study also showed a decreasing trend in the 10-DAB treatment groups (compared with the Control group), suggesting that 10-DAB may also have a certain ameliorative effect on the splenomegaly (an indicator of over-activation of the immune system) associated with AIA mice (**Figure 1C and D**).

Collectively, high-dose 10-DAB conferred significant anti-arthritic activity in AIA mice, as evidenced by marked suppression of joint edema, improvement in clinical arthritis scores, and reduction of the spleen index, collectively highlighting its therapeutic potential.

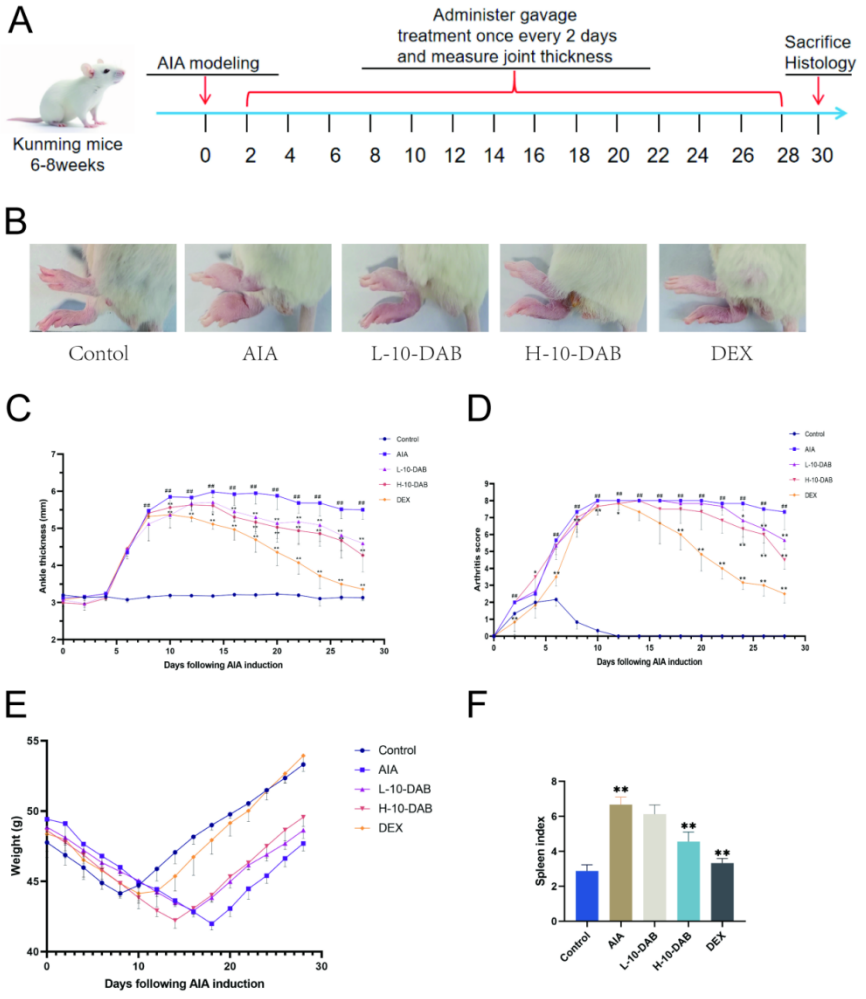

Figure 1. 10-DAB ameliorates AIA-induced inflammation and systemic morbidity.
Experimental timeline. (B) Representative photographs of ankle joints on day 28. (C) Time-course of hind-paw thickness (Δ mm vs baseline). (D) Clinical arthritis score (0–12 scale). (E) Body-weight changes during treatment. (F) Spleen index (mg g^{-1}) at termination (day 28). Data are mean ± SD, n = 6 per group. #P < 0.05, ##P < 0.01, ###P < 0.001 vs Control; *P < 0.05, **P < 0.01, ***P < 0.001 vs AIA (one-way ANOVA followed by Tukey's post-hoc test).

3.2. 10-DAB improves the pathological changes in joint tissue sections of AIA mice

To evaluate the protective effect of 10-DAB on pathological alterations and bone destruction in the joints of AIA mice, we conducted H&E staining and TRAP staining on knee joint tissue sections [19]. The changes in knee joint pathological features (**Figure 2A**) are as follows: The Control group exhibited intact knee joint tissue structure, with no inflammatory cell infiltration in the synovium, no pannus formation, and no bone erosion, indicating no significant pathological changes. The AIA group showed severe synovial hyperplasia (which had invaded the joint cavity) accompanied by significant inflammatory cell infiltration, suggesting the successful establishment of the AIA model. After intervention with different concentrations of 10-DAB, there was a trend of improvement in pathological changes: The L-10-DAB group continued to exhibit synovial hyperplasia and moderate inflammatory cell infiltration, along with mild bone damage (less severe than that in the AIA group). The H-10-DAB group showed intact bone tissue structure, with the disappearance of synovial hyperplasia and inflammatory cell infiltration. The DEX group demonstrated a reduction in the degree of synovial thickening and inflammatory cell infiltration.

TRAP, a selective hydrolase of osteoclasts, was exploited to map active resorptive sites. Control knees contained only sporadic TRAP-positive multinucleated cells located at the chondro-osseous junction, and the subchondral plate

remained smooth and intact (**Figure 2B**). In contrast, AIA sections revealed a dense, diffuse band of osteoclasts carpeting the articular surface, extending into the subchondral bone and marrow cavity; concomitant cortical discontinuities and trabecular perforations were evident. 10-DAB administration dose-dependently contracted this TRAP-positive population and narrowed its territorial distribution, paralleling the attenuation of osteolytic lesions.

Collectively, these data demonstrate that 10-DAB suppresses synovial inflammation and curtails osteoclast genesis in AIA mice, thereby limiting structural joint damage.

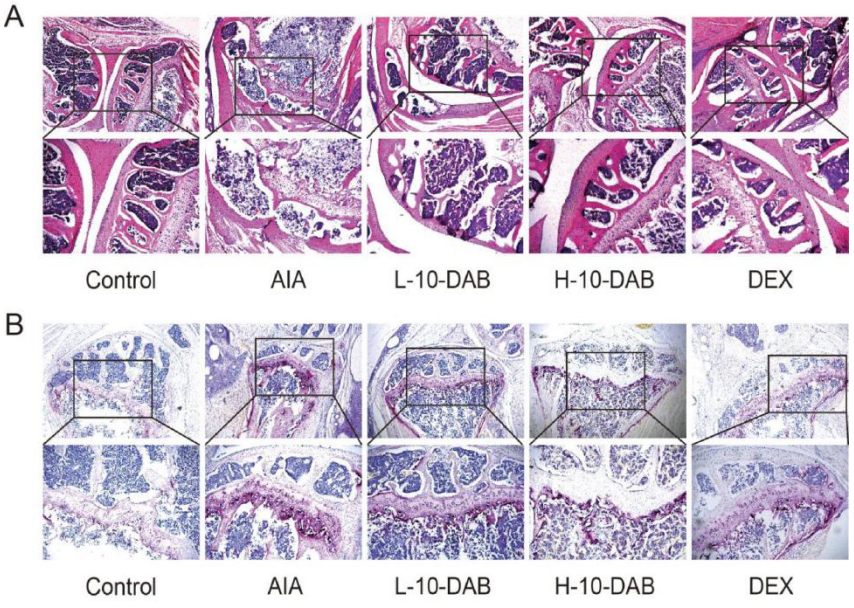

Figure 2. Histopathological assessment of knee joints.
Haematoxylum–eosin (H&E) staining: evaluation of synovial hyperplasia, inflammatory infiltration, and cartilage/bone integrity. (B) Tartrate-resistant acid phosphatase (TRAP) staining: localization of osteoclasts (red-purple precipitation) at the articular surface and subchondral bone.

3.3. Effect of 10-DAB on Serum Cytokine Levels in AIA Mice

To determine whether 10-DAB acts via humoral immune modulation, serum IL-6, TNF-α and IL-10 were quantified by ELISA (5-fold dilution, uniform across samples). Compared with controls, AIA mice exhibited a marked rise in IL-6 and TNF-α and a concomitant fall in IL-10, confirming a systemic pro-inflammatory shift. High-dose 10-DAB (H-10-DAB) significantly reversed these changes. Low-dose 10-DAB (L-10-DAB) did not achieve statistical significance for any cytokine. Dexamethasone mirrored the inhibitory effect of H-10-DAB on IL-6 and TNF-α but failed to elevate IL-10. These findings collectively indicate that high-dose 10-DAB effectively suppresses the release of pro-inflammatory cytokines (IL-6 and TNF-α) while partially restoring anti-inflammatory IL-10 expression. This suggests that 10-DAB mitigates inflammation by bidirectional modulation of the cytokine network, thereby restoring immune balance in AIA mice.

3.4. 10-DAB Suppresses Splenic NF-κB Activation in AIA Mice in a Dose-dependent Manner

Based on our previous findings that 10-DAB ameliorates arthritis symptoms in AIA mice (including arthritis scores, histopathological changes, and serum inflammatory cytokine levels), we further investigated whether 10-DAB exerts its effects by modulating the NF-κB signaling pathway. The NF-κB pathway plays a pivotal role in inflammatory responses and immune cell differentiation [20]. Western blotting was employed to assess the expression levels of NF-κB signaling pathway-related proteins, specifically the phosphorylation levels of IκBα and p65 **(Figure 4)**. In the Control group, mice exhibited low expression levels of phosphorylated IκBα and p65 in the spleen. Compared to the Control group, the AIA group demonstrated a significant increase in the phosphorylation of both IκBα and p65. In AIA mice treated with low-dose

10-DAB, although a reduction in splenic IκBα and p65 phosphorylation levels was observed, the difference did not reach statistical significance compared to the AIA group. Conversely, high-dose 10-DAB treatment significantly suppressed p65 phosphorylation and markedly reduced IκBα phosphorylation. Additionally, dexamethasone (DEX), used as a positive control, also significantly inhibited the phosphorylation of both p65 and IκBα. Thus, 10-DAB dose-dependently restrains NF-κB activation, providing a mechanistic basis for its anti-arthritic action.

3.5. 10-DAB Attenuates the Expression Levels of Inflammatory Factors in the Spleen of AIA Mice

Our previous studies demonstrated that 10-DAB effectively inhibits NF-κB signalling in the spleens of AIA mice. Here we extended this observation to two downstream effectors, inducible nitric-oxide synthase (iNOS) and matrix metalloproteinase-3 (MMP-3) [21], that drive inflammatory amplification and cartilage degradation in rheumatoid arthritis. Western blot analysis of splenic lysates revealed robust up-regulation of both iNOS and MMP-3 in AIA mice. 10-DAB pretreatment dose-dependently suppressed the expression of these proteins, indicating that 10-DAB not only blocks NF-κB activation but also attenuates its downstream inflammatory and catabolic mediators, thereby providing further mechanistic insight into the amelioration of joint inflammation and cartilage destruction in RA.

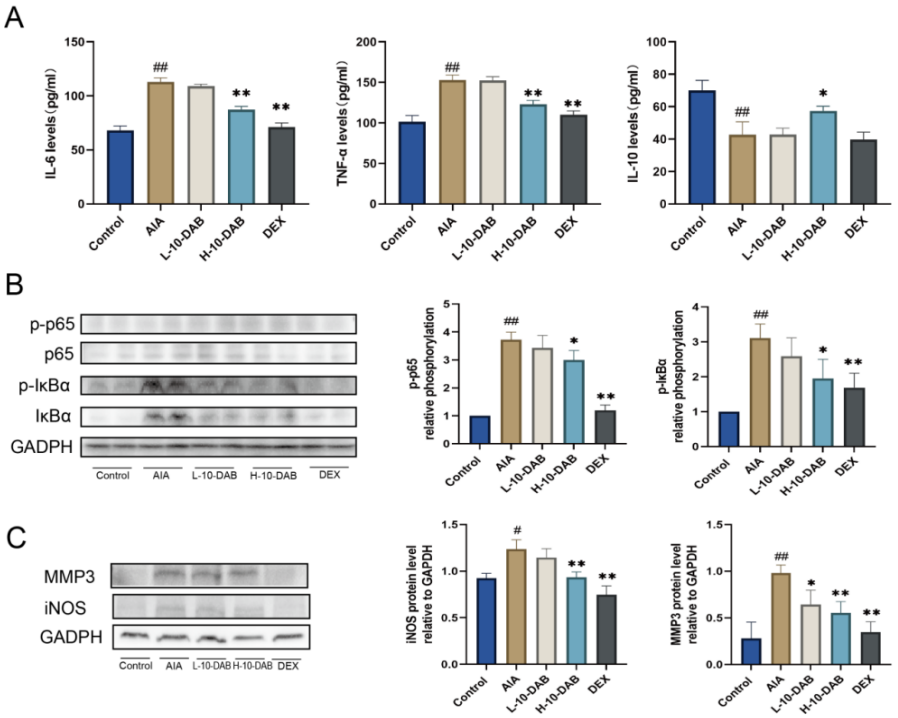

Figure 3. (A) 10-DAB dose-dependently restored the dysregulated serum cytokine signature in AIA mice. (B) 10-DAB significantly attenuated phosphorylation of p65 and IκBα in splenic lysates. (C) Expression of the downstream NF-κB–dependent inflammatory effectors MMP-3 and iNOS was markedly down-regulated by 10-DAB. Data are expressed as mean ± SD. Significance versus Control: #P < 0.05, ##P < 0.01, ### P < 0.001; significance versus AIA: *P < 0.05, **P < 0.01, ***P < 0.001 (one-way ANOVA followed by Tukey's post-hoc test).

3.6. 10-DAB Exerts Anti-inflammatory Effects in LPS-Induced Macrophages by Inhibiting NF-κB Phosphorylation

In vitro, to investigate whether 10-DAB exerts anti-inflammatory effects through modulation of the NF-κB signaling pathway, we conducted a series of intervention studies using LPS-induced RAW264.7 macrophages as a model. First, drug safety was evaluated using the CCK-8 assay, which revealed that 10-DAB, at concentrations up to 10 μM, exhibited no cytotoxic effects on LPS-stimulated macrophages and even promoted cell proliferation in a concentration-dependent manner. Therefore, we selected two concentrations, 2.5 μM and 10 μM, for subsequent experiments, with dexamethasone

(DEX, 0.5 μM) serving as a positive control—a concentration also confirmed to have no significant cytotoxic effects on the cells.

In this study, RAW264.7 macrophages were stimulated with LPS (500 ng mL^{-1}) for 12 h to establish an in vitro inflammation model, followed by 24 h treatment with graded concentrations of 10-DAB or dexamethasone (DEX)[22]. Whole-cell lysates were then subjected to Western blot analysis to determine the phosphorylation status of the NF-κB signaling core proteins IκBα and p65.

Control cells exhibited barely detectable levels of phospho-IκBα (p-IκBα) and phospho-p65 (p-p65). LPS challenge markedly elevated the phosphorylation of both targets. Low-dose 10-DAB (2.5 μmol mL^{-1}) modestly reduced p-IκBα and p-p65 signals, but the decrease did not reach statistical significance relative to the LPS group. In contrast, high-dose 10-DAB (10 μmol mL^{-1}) significantly suppressed p-p65 and p-IκBα phosphorylation. DEX, employed as a positive control, produced a comparable inhibitory effect on both p-p65 and p-IκBα.

Collectively, these data demonstrate that 10-DAB concentration-dependently inhibits LPS-induced phosphorylation of the NF-κB signaling axis, providing a key molecular basis for its anti-inflammatory activity.

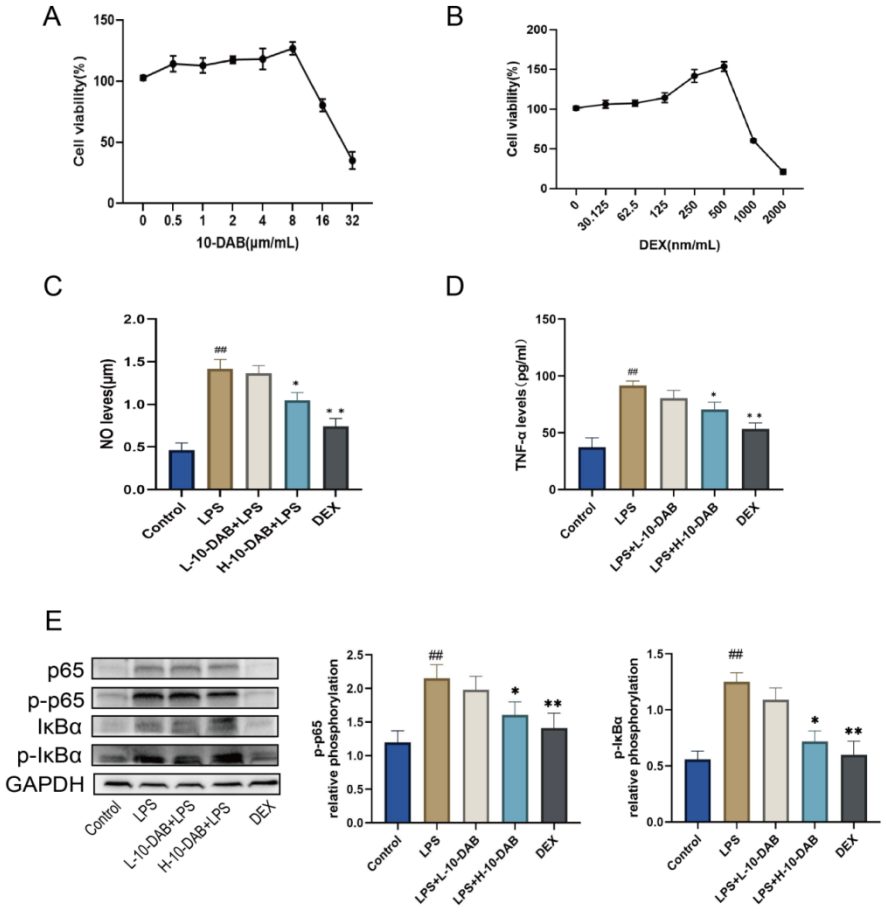

Figure 4. (A)10-DAB lacked cytotoxicity in LPS-stimulated macrophages in CCK-8 assays. (B) DEX exhibited no cytotoxicity under identical conditions in CCK-8 assays. (C)10-DAB dose-dependently suppressed LPS-driven NO release. (D)10-DAB dose-dependently inhibited LPS-induced TNF-α secretion. (E)10-DAB blunted LPS-evoked phosphorylation of p65 and IκBα, indicating NF-κB pathway targeting. Values are mean ± SD. #P < 0.05, ##P < 0.01, ###P < 0.001 versus untreated control; *P < 0.05, **P < 0.01, ***P < 0.001 versus LPS-alone group.

4. Discussion

By integrating in-vivo AIA-model data with in-vitro macrophage assays, we show that 10-DAB ameliorates arthritis chiefly through blockade of NF-κB signaling, and thus offer both mechanistic rationale and pre-clinical proof-of-concept

for its development as a novel RA therapeutic.

First, the central finding of this study is the identification of NF-κB as the principal molecular target of 10-DAB. Consistent data from both in-vivo AIA mice and in-vitro macrophages demonstrate that 10-DAB effectively suppresses the critical activation events of the NF-κB signaling cascade. Accordingly, splenic lysates from AIA mice receiving 10-DAB displayed markedly attenuated p-IκBα and p-p65 levels, accompanied by impaired p65 nuclear translocation. Parallel in-vitro experiments further revealed that 10-DAB dose-dependently blunted LPS-induced phosphorylation of both IκBα and p65 in RAW264.7 macrophages, corroborating the NF-κB inhibitory profile observed in vivo. Collectively, these congruent in-vivo and in-vita data establish NF-κB blockade as the proximal anti-inflammatory mechanism of 10-DAB [23], providing a mechanistic rationale—consistent with the documented contribution of NF-κB to cytokine overproduction by macrophages in RA—for its therapeutic efficacy in rheumatoid arthritis.

Second, we identify macrophages as the principal effector population through which 10-DAB confers protection. Synovial tissue of RA patients is densely infiltrated by activated macrophages that release TNF-α, IL-1β and other cartilage-destructive mediators [24]. Accordingly, we employed RAW264.7 macrophages—a widely accepted in-vitro surrogate of synovial macrophages—to dissect the underlying mechanism. The results revealed that 10-DAB directly targets macrophages, suppressing TNF-α and other inflammatory mediators by blocking NF-κB activation. Hence, the in-vivo efficacy of 10-DAB is, at least in part, attributable to its direct suppression of macrophage hyperactivation.

Third, this study highlights the multi-faceted benefits of 10-DAB. Beyond suppressing pro-inflammatory cytokines, we observed that 10-DAB downregulates downstream effector molecules such as iNOS and MMP-3. Excessive NO generated by iNOS exhibits cytotoxicity, while MMP-3 directly degrades cartilage matrix [25]. Thus, by inhibiting NF-κB upstream, 10-DAB likely achieves dual therapeutic effects: anti-inflammatory and joint-protective. Furthermore, the natural origin of 10-DAB confers unique advantages.

As a precursor of paclitaxel, it is relatively abundant in plant sources. Our CCK-8 assays confirmed no cytotoxicity at effective concentrations, suggesting a favorable safety profile. Although its potency in vitro is slightly lower than that of dexamethasone (DEX), the severe side effects associated with long-term DEX use underscore the importance of developing natural alternatives like 10-DAB—with well-defined mechanisms and potentially superior safety—for long-term RA management.

Notably, this study has limitations. For instance, while we confirmed NF-κB pathway inhibition by 10-DAB, its direct molecular targets (e.g., inhibition of IKK or upstream receptors) remain to be identified. Additionally, future studies should focus on the pharmacokinetic profile of 10-DAB in RA models and its indirect effects on adaptive immunity (e.g., T and B cells).

In summary, this study provides compelling evidence that the natural compound 10-DAB alleviates CFA-induced arthritis by suppressing NF-κB activation in macrophages, with mechanisms involving reduced pro-inflammatory cytokine release and inhibition of joint-destructive factors. These findings deepen understanding of 10-DAB's pharmacological properties and strengthen its candidacy as a promising, nature-derived therapeutic for RA. Future research should prioritize optimization of its derivatives, precise molecular target identification, and evaluation of its clinical translation potential.

Funding

This work was supported by the Basic Scientific Research Operating Funds of Guilin Medical University.

Disclosure statement

The author declares no conflict of interest.

References

[1] Li X, Yang Y, Sun G , et al., 2020, Promising Targets and Drugs in Rheumatoid Arthritis: A Module-based and Cumulatively Scoring Approach. Bone Joint Res., 9(8):501-514.

[2] Chen M, Fu W, Xu H, et al., 2023, Tau Deficiency Inhibits Classically Activated Macrophage Polarization and Protects against Collagen-induced Arthritis in Mice. Arthritis Res Ther., 25(1):146.

[3] Ding Q, Hu W, Wang R, et al., 2023, Signaling Pathways in Rheumatoid Arthritis: Implications for Targeted Therapy. Signal Transduct Target Ther., 8(1):68.

[4] Meng M, Yao J, Zhang YK, et al., 2023, Potential Anti-Rheumatoid Arthritis Activities and Mechanisms of Ganoderma Lucidum Polysaccharides. Molecules., 28(6):2483.

[5] Kciuk M, Garg A, Rohilla M, et al., 2024, Therapeutic Potential of Plant-Derived Compounds and Plant Extracts in Rheumatoid Arthritis-Comprehensive Review. Antioxidants (Basel)., 13(7):775.

[6] An Z, Qin J, Bo WB, et al., 2022, Prognostic Value of Serum Interleukin-6, NF-κB plus MCP-1 Assay in Patients with Diabetic Nephropathy. Dis Markers., 2022:4428484.

[7] Ge C, Ma C, Cui JS, et al., 2023, Rapamycin Suppresses Inflammation and Increases the Interaction between p65 and IκBα in Rapamycin-induced Fatty Livers. PLoS One., 18(3):e0281888.

[8] Oh E, Jang H, Ok S, et al., 2023, WGA-M001, a Mixture of Total Extracts of Tagetes erecta and Ocimum basilicum, Synergistically Alleviates Cartilage Destruction by Inhibiting ERK and NF-κB Signaling. Int J Mol Sci., 24(24):17459.

[9] Park SU, Ahn DJ, Jeon HJ, et al., 2012, Increase in the Contents of Ginsenosides in Raw Ginseng Roots in Response to Exposure to 450 and 470 nm Light from Light-Emitting Diodes. J Ginseng Res., 36(2): 198-204.

[10] Li S, Zhang P, Zhang M, et al., 2013, Functional Analysis of a WRKY Transcription Factor Involved in Transcriptional Activation of the DBAT Gene in Taxus Chinensis. Plant Biol (Stuttg)., 15(1):19-26.

[11] Qayum M, Nisar M, Shah MR, et al., 2012, Analgesic and Antiinflammatory Activities of Taxoids from Taxus Wallichiana Zucc. Phytother Res., 26(4):552-6.

[12] Georgopoulou K, Smirlis D, Bisti S, et al., 2007, In Vitro Activity of 10-deacetylbaccatin III against Leishmania Donovani Promastigotes and Intracellular Amastigotes. Planta Med., 73(10):1081-8.

[13] Honmore VS, Kandhare AD, Kadam PP, et al., 2019, Diarylheptanoid, A Constituent Isolated from Methanol Extract of Alpinia Officinarum Attenuates TNF-α Level in Freund's Complete Adjuvant-induced Arthritis in Rats. J Ethnopharmacol., 229:233-245.

[14] Quan LD, Thiele GM, Tian J, et al., 2008, The Development of Novel Therapies for Rheumatoid Arthritis. Expert Opin Ther Pat. 2008 Jul;18(7):723-738.

[15] Chen Y, Zeng B, Shi P, et al., 2019, Comparative Analysis of the Liver and Spleen Transcriptomes between Holstein and Yunnan Humped Cattle. Animals (Basel)., 9(8):527.

[16] Wu Z, Xu L, He Y, et al., 2020, DUSP5 suppresses interleukin-1β-induced chondrocyte inflammation and ameliorates osteoarthritis in rats. Aging (Albany NY)., 12(24):26029-26046.

[17] Ciemniecki JA, Lewis CP, Gupton JT, et al., 2016, Effects of A Pyrrole-based, Microtubule-depolymerizing Compound on RAW 264.7 Macrophages. Chem Biol Interact., 246:63-8.

[18] Swanson CD, Akama-Garren EH, Stein EA, et al., 2012, Inhibition of Epidermal Growth Factor Receptor Tyrosine Kinase Ameliorates Collagen-induced Arthritis. J Immunol., 188(7):3513-21.

[19] Luo Y, Xiang Y, Lu B, et al., 2023, Association between dietary selenium intake and the prevalence of osteoporosis and its role in the treatment of glucocorticoid-induced osteoporosis. J Orthop Surg Res. 2023 Nov 15;18(1):867.

[20] Liu G, Li D, Zhang L, et al., 2022, Phenformin Down-Regulates c-Myc Expression to Suppress the Expression of Pro-Inflammatory Cytokines in Keratinocytes. Cells., 11(15):2429.

[21] Li Q, Zhao X, Wang A, et al., 2025, From Molecular Mechanism to Plant Intervention: the Bidirectional Regulation of Inflammation and Oxidative Stress in Bone Aging. Front Endocrinol (Lausanne)., 16:1634580.

[22] Wu M, Ding H, Tang X, et al., 2023, Efficiency of A Novel Thermosensitive Enema in Situ Hydrogel Carrying Periplaneta

Americana Extracts for the Treatment of Ulcerative Colitis. Front Pharmacol., 14:1111267.

[23] Mei K, Chen Z, Wang Q, et al., 2023, The Role of Intestinal Immune Cells and Matrix Metalloproteinases in Inflammatory Bowel Disease. Front Immunol., 13:1067950.

[24] Chen X, Zhou B, Gao Y, et al., 2022, Efficient Treatment of Rheumatoid Arthritis by Degradable LPCE Nano-Conjugate-Delivered p65 siRNA. Pharmaceutics., 14(1):162.

[25] Georget M, Defois A, Guiho R, et al., 2023, Development of A DNA Damage-induced Senescence Model in Osteoarthritic Chondrocytes. Aging (Albany NY)., 15(17):8576-8593.